Total Absorption Spectroscopy for the β^+ decay strength distribution of ^{60}Ga

G. Owens-Fryar,[1,2,*] S. M. Lyons,[3,4,†] A. L. Richard,[1,4,5] A. Spyrou,[1,2,4] B. A. Brown,[1,2] C. E. P. Robin,[6,7] Z. Meisel,[4,5] H. C. Berg,[1,2,4,8] A. Chester,[1,4] A. A. Chen,[9] B. Crider,[10] P. A. DeYoung,[4,11] P. Gastis,[12] E. C. Good,[1,4,†] C. Harris,[1,2,4] K. Hermansen,[1,2] S. N. Liddick,[1,13] W. J. Ong,[14] A. Palmisano-Kyle,[1,2,4] A. Psaltis,[9,15,16] M. K. Smith,[1] E. Rubino,[17] S. K. Subedi,[18] I. Sultana,[5] and A. Tsantiri[1,2,4]

[1] *Facility for Rare Isotope Beams, East Lansing, MI 48824 USA*
[2] *Department of Physics and Astronomy, Michigan State University, East Lansing, MI 48824 USA*
[3] *National Superconducting Cyclotron Laboratory, East Lansing, MI 48824 USA*
[4] *Joint Institute for Nuclear Astrophysics - Center for the Evolution of the Elements East Lansing, MI 48824 USA*
[5] *Ohio University, Athens, OH 45701 USA*
[6] *Fakultät für Physik, Universität Bielefeld, D-33615, Bielefeld, Germany*
[7] *GSI Helmholtzzentrum für Schwerionenforschung, Planckstraße 1, 64291 Darmstadt, Germany*
[8] *University of Oslo, N-0316 Oslo, Norway*
[9] *Department of Physics and Astronomy, McMaster University, Hamilton, Ontario L8S 4M1, Canada*
[10] *Mississippi State University, Mississippi State, MS 39762 USA*
[11] *Hope College, Holland, MI 49423 USA*
[12] *Central Michigan University, Mount Pleasant, MI 48859 USA*
[13] *Department of Chemistry, Michigan State University, East Lansing, MI 48824 USA*
[14] *Lawrence Livermore National Laboratory, Livermore, CA 94550*
[15] *Triangle Universities Nuclear Laboratory, Duke University, Durham, NC, 27710, USA*
[16] *Department of Physics, Duke University, Durham, NC, 27710, USA*
[17] *Florida State University, Tallahassee, FL 32306*
[18] *Ohio University, Athens, OH 45701 USA*

(Dated: April 15, 2025)

β-decay properties play an important role in most astrophysical processes. In the absence of experimental data, astrophysical models rely on global theoretical calculations to provide the relevant properties. It is therefore important to provide strong experimental constraints when possible. In the case of β-decay, the most sensitive probe is the β-decay strength distribution. We report here on the first measurement of the latter quantity for the β^+ decay of ^{60}Ga using the total absorption spectroscopy technique. The experimental results are compared to theoretical calculations often used in astrophysical models, namely the shell model and the quasi-particle random phase approximation (QRPA), as well as an extension of QRPA that includes higher-order nucleonic calculations. Both models are in reasonable agreement with the experimental results.

Keywords: Neutron Deficient Isotope, Total Absorption Spectroscopy, Gamow-Teller Transition Strength, β-decay Feeding Intensity

I. INTRODUCTION

One of the goals of nuclear astrophysics is to understand the various astrophysical events occurring in the cosmos. One such event, type I X-ray bursts (XRB1), is one of the most common explosive events in the galaxy [1–4]. They are widely accepted to result from neutron stars accreting mass from a partner star in a binary system. In a binary system, hydrogen and helium are pulled onto the surface of the neutron star from its partner star. As the material builds up on the surface, the rise in temperature and density reach conditions for a thermonuclear runaway, which results in a XRB1. XRB1s are of particular interest because they provide insight into the behavior of high density matter in an unrelenting environment [2, 3].

The abundance outputs of astrophysical models of XRB1s depend strongly on several nuclear reaction rates, occurring both on the surface and inside the crust of neutron stars by the buried ashes. This process is called the rapid proton (rp) capture process. The rp process is dominated by the competition between proton capture reactions and β^+ decays. By investigating the rp process, the dynamics of neutron stars and features of XRB1 spectra can be better understood. Sensitivity studies have shown that the nuclear properties within the rp process have a significant impact on the light curve of the XRB1 [5–7]. When experimental data are absent, astrophysical calculations rely on theoretical models to provide the necessary nuclear input. Here we focus in particular on β^+ decays. β-decay properties used in astrophysical calculations are often calculated using the Shell Model [8–10] where available, and the Quasi-particle Random Phase Approximation (QRPA) [11]. Typically, these models are validated with β-decay half-lives. However, β-decay half-lives are calculated within these models by integrating the β-decay strength distribution as a function of excita-

* owensfry@frib.msu.edu
† currently at Pacific Northwest National Laboratory

tion energy. Therefore, a more sensitive test of the theoretical models is the direct comparison of the β-decay strength distribution to experimental data [12–15].

Here, we present the first complete measurement of the β-decay feeding intensity (I_β) of ^{60}Ga. This decay was studied previously using high-resolution γ-ray spectroscopy [16]. Such measurements, while ideal for identifying low-lying discrete states and their corresponding γ-ray emission, are known to suffer from the so-called "pandemonium effect" [17]. This term refers to the phenomenon where the β-decay feeding intensity into low energy states is overestimated, while the feeding into high energy states is underestimated or missing completely. The pandemonium effect is a result of the limited detection efficiency of high-resolution systems, and can be overcome when using a γ-ray total absorption spectrometer (TAS) (e.g. Refs. [13, 18, 19]). Here we apply the TAS method for the first time to the β^+ decay of ^{60}Ga and compare the experimental results to models commonly used in astrophysical calculations, namely the Shell Model and QRPA.

II. EXPERIMENTAL DETAILS

The experiment was performed at the National Superconducting Cyclotron Laboratory. A 150 MeV/u ^{78}Kr^{36+} primary beam impinged on a 517 mg/cm^2 ^{9}Be target to produce the isotope of interest. The projectile fragments were filtered by the A1900 separator [20]. The fragment separator had a broad momentum acceptance, so a " cocktail" beam of isotopes around A=55 reached the detector set-up [12]. To remove further contamination, the radio frequency fragment separator (RFFS) was utilized [21]. The RFFS removed low momentum tails of more abundant nuclei to have better selection for neutron-deficient isotopes.

The isotopes in the cocktail beam were identified using time-of-flight and energy loss data from a group of detectors upstream of the experimental set-up. This detector group consisted of one plastic scintillator in the focal plane of the A1900 providing timing information and two thin silicon PIN detectors located just upstream of the implantation station, each recording energy loss and time[20]. The particle identification is shown in Fig. 1.

The experimental set-up incorporated the Summing NaI(Tl) (SuN) detector [22] and a Double Sided Silicon Strip Detector (DSSD) placed in the center of the bore hole of SuN [12] as an implantation surface. Following the DSSD, a silicon surface barrier veto detector capped off the beam line to detect any contaminants not stopped in the DSSD [14]. The details of this setup can be found in [23]; here we summarize the key features.
SuN is a segmented, high-efficiency, 4π γ-ray calorimeter. It is 16 in. in diameter, 16 in. long, and has a 1.8 in. diameter bore hole along the beam axis. There are eight optically isolated NaI(Tl) scintillator segments; four along the length of SuN on both the top and bottom halves, with three photomultiplier tubes (PMTs) on each crystal. SuN has an angular coverage of 98% at its center with peak efficiency for 661 keV γ-ray of ^{137}Cs at 85(2)%
.

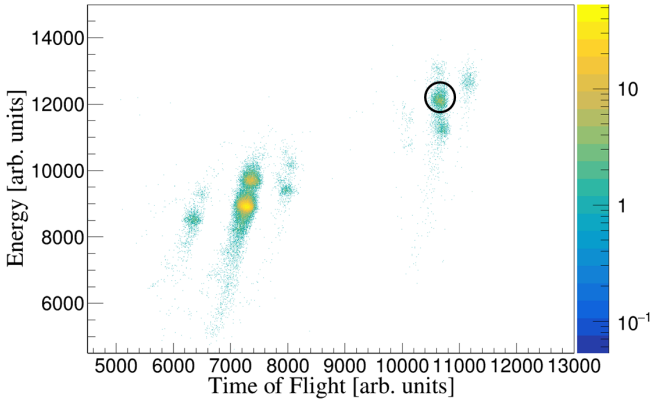

FIG. 1. Particle identification plot of the "cocktail" beam delivered to the experiment area. The isotope of interest, ^{60}Ga, is circled in black.

The DSSD placed in the center of SuN was 1-mm thick, with 32 1.2-mm wide strips in total; 16 strips on each side, the front strips being perpendicular to the back strips. The resultant DSSD signals passed through dual gain preamplifiers, enabling simultaneous detection of the implanted ions and β-decay positrons. This allowed the data to be correlated in space and time, so the implant event could be matched to its decay event.
Different γ-ray spectra can be taken with SuN. The TAS spectrum illustrates the total energy level of the child nucleus populated by β-decay. In a TAS spectrum, SuN is treated as one large, continuous detector. In addition, the spectra from the individual crystals can be added together to create a single Sum of Segments (SoS) spectrum. This spectrum was used to analyze the de-excitation of single levels by γ emission. The multiplicity is the number of crystals that detect energy above the threshold during an event. Multiplicity spectra were used to understand how many γ-rays were observed during the de-excitation of the child nuclei.

III. ANALYSIS

Implantation and β-decay events were correlated within a 400 ms time window. This time window was chosen because it was large in comparison to previously measured half-lives, minimized uncorrelated data, and maximized real correlations. Events fulfilling criteria for each type of event were separated for analysis. An im-

plantation event was defined by having signals in both PIN detectors, and at least one strip on both sides of the DSSD in low gain. A decay event was defined by having no signal in either PIN detector, but a signal in both sides of the DSSD in high gain. The implantation and decay pixels were determined by the front and back strip with the maximum energy during the respective events. Once identified, the decay events were correlated with the implantation events. First, a decay event and implantation events in the time window within the same pixel were identified (real correlations). There is no guarantee that the selected decay event is coming from the particular ion with which it was correlated. Decays from other ions are also included in these "real correlations". To account for this, random correlation spectra were also generated by grouping decay events that occurred before their corresponding implantation events within the specified time window (random correlations). The random correlation spectra were then subtracted from the real correlation spectra.

In order to extract the β-decay feeding intensity at the various excitation energies, the detector response had to be accounted for. This was done using a GEANT4 [24] simulation of the detector geometry and response of the setup for the measured decay [22, 24, 25], taking into account the experimental β-decay Q-value of 13.56 MeV [26]. In GEANT4, the energy of electrons, positrons, and γ-rays were tracked and recorded into spectra analogous to the experimental spectra. First, the de-excitation of discrete states of the child nucleus from the RIPL-3 library [27] were simulated individually using GEANT4. Then, the de-excitation of continuum states of the child nuclei were simulated with the Monte Carlo simulation code RAINIER [28]. RAINIER assumes the RIPL-3 level scheme is complete up to an energy defined by the user. In this work, the level scheme was assumed complete up to 4.9 MeV to include all known states with energies below the proton separation energy of 5.1 MeV. Above this energy, it created a simulated level scheme of the child nucleus based on a user-defined level density model. Here, the continuum region simulations were created using the Constant Temperature model [29, 30] assuming a spin distribution from rigid sphere nucleus model [31]. The user also needs to define the initial excitation energy and J^π and select a γ-ray strength function model. For this experiment, the excitation energies were a sample of continuum state energies from just above the discrete region to the Q-value of the decay, with energy steps that followed the energy resolution of the SuN detector. The γ-ray strength function was described with a generalized Lorentzian distribution [32]. It should be noted that the aforementioned statistical properties affect only the detector efficiency estimate (which has a 10% uncertainty [22]). Therefore the β-decay feeding intensity when varying these properties is consistent within the total uncertainty of our results. The RAINIER output was then converted to GEANT4 input files for each excitation energy. Each of these simulated components, together with the discrete levels, output TAS, SoS, and multiplicity spectra. A χ^2 minimization was performed to extract the β-feeding intensity of each level, simultaneously fitting the experimental TAS, SoS, and multiplicity spectra as shown in Fig. 2. The best fit had a reduced χ^2 of 1.37. This technique has been previously applied to study β^- decays [12–14, 33].

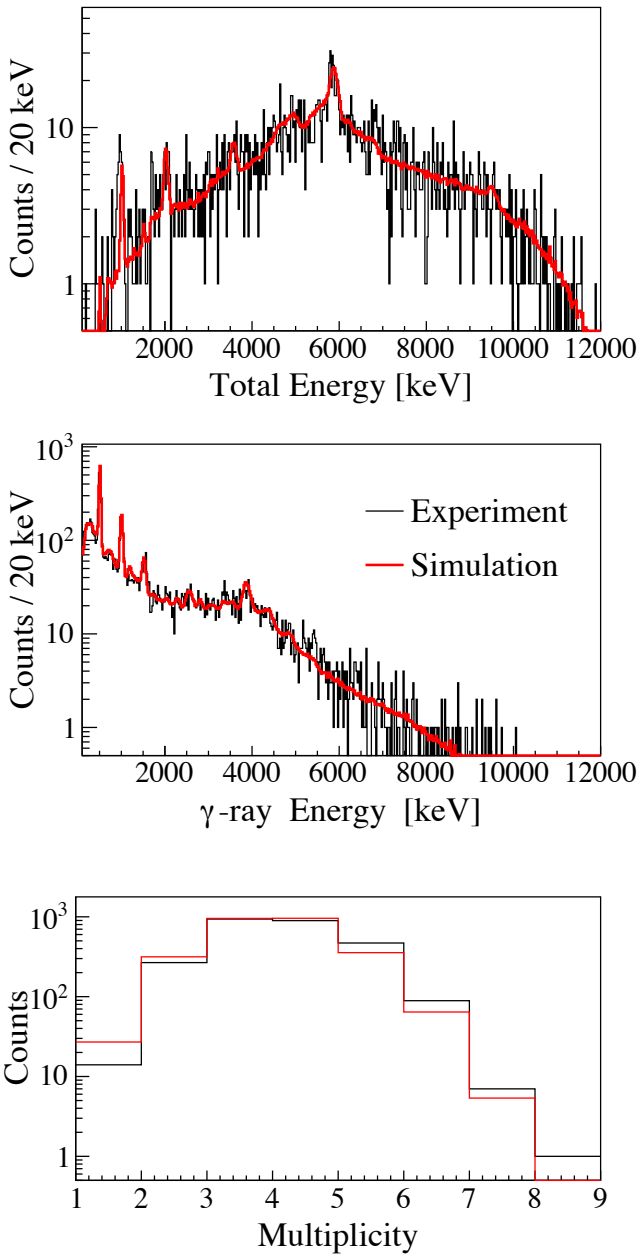

FIG. 2. A χ^2 fit of a typical : a. Total Absorption Spectrum (TAS) , b. Sum of Segments and c. Multiplicity. The experimental results are shown in black and the line of best fit is in red.

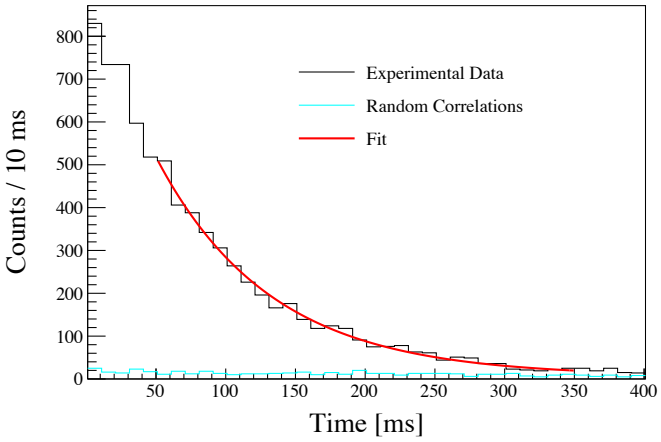

FIG. 3. Fit of the ^{60}Ga decay half-life. The black line shows number of events detected over time. The cyan line shows random correlations which serves as a background. The red line is an exponential + linear fit of the data.

IV. RESULTS

A. Half-Life

The β-decay half-life of ^{60}Ga was measured by tracking the time between the implant event and the correlated decay event. From this, a decay curve was extracted as shown in Fig.3 and was fit with an exponential function with a linear background. The extracted half-life of 57.7 $\pm$ 9.8 ms can be compared with previously measured values of 70$\pm$ 15 ms [16], 69.4 $\pm$ 2 ms [34] and 76 $\pm$ 3 ms [35]. The estimated uncertainty was determined by calculating the standard deviation of multiple fits performed across the correlation window.

B. Total Absorption Spectroscopy

Experimental spectra from the decay of ^{60}Ga are presented in Fig. 2. From the simultaneous χ^2 fit of the three experimental spectra, the feeding intensities of each excitation energy component were extracted and normalized to 100% (Fig.4 and Table I). The uncertainty band includes: varying spins for states with uncertain spin assignments, statistical uncertainty, detector efficiency, the fit uncertainty, as well as the differences between the average to the maximum and minimum I_β calculated at each energy.

To vary the states without known spin assignments, several copies of the RIPL-3 [27] input file were made varying the spin and parity (J^π) values. The simulation process was repeated for each of these inputs as a part of the error analysis. The final I_β values for each excitation energy bin are shown in Table. I, together with the upper and lower limits of the uncertainty estimate. We recognize that the uncertainty for some energies is large compared to the measurement. This arises from the fact that for some of the variations particular energy bins appeared with zero values of the I_β. While it is not immediately clear why such differences are present, we include the extreme limits for completeness. In the future, when firm spin assignments are available, this analysis could be repeated to improve its accuracy. The data show that there is an I_β intensity of 12.8% above the proton separation energy. The isobaric analogue state (IAS) is shown in Fig.4 as the dramatic increase in β feeding percentage. The intensity was then converted to Gamow-Teller transition strength (B(GT)) with the method used in [12, 15] as shown in Fig. 6. For a consistent comparison to theory, the substantial contribution from the Fermi transition of the 4.85 MeV IAS was removed from the total experimental Gamow-Teller transition strength.

TABLE I. Table listing I_β values at each energy level included in the χ^2 minimization along with the average of the uncertainties above and below the distribution. Intensities below 1e-3 are set to zero due to sensitivity limitations.

Energy[keV]	Iβ[%]	Upper Limit[%]	Lower Limit[%]
0	3.8	4.4	3.2
1 004	0.2	1.5	0.0
2 193	0.0	0.0	0.0
2 559	7.8	8.8	6.6
3 035	0.4	0.7	0.0
3 200	0.0	0.0	0.0
3 510	2.1	2.7	1.4
3 627	5.8	6.9	4.6
3 710	0.0	0.0	0.0
3 808	0.0	0.0	0.0
3 812	5.3	6.7	0.1
3 972	8.6	11.4	7.0
4 180	0.0	0.0	0.0
4 200	0.0	0.0	0.0
4 351	0.0	0.0	0.0
4 400	0.0	0.0	0.0
4 776	0.0	0.0	0.0
4 852	37.7	45.2	33.0
4 913	11.0	13.2	6.9
5 200	4.7	6.2	0.0
5 460	3.1	5.2	2.3
5 733	4.9	6.2	0.0
6 020	1.0	8.4	0.0
6 321	0.0	0.0	0.0
6 637	0.1	1.0	0.0
6 969	0.0	0.0	0.0
7 317	0.0	0.0	0.0
7 683	0.0	0.3	0.0
8 067	0.0	0.0	0.0
8 470	1.7	3.0	0.6
8 894	0.1	0.5	0.0
9 338	1.2	2.1	0.0
9 805	0.5	1.8	0.1

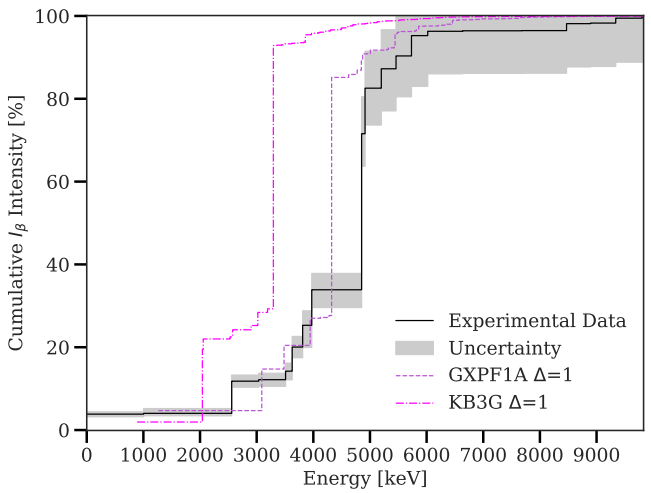

FIG. 4. Cumulative I_β of measurement compared to various Shell Model Hamiltonians. Despite disagreements in energy, the overall shape of the various sets is consistent. The I_β at each energy is listed in Table I

C. Shell Model Calculations

Calculations for the β-decay of ^{60}Ga were carried out within the $(0f_{7/2}, 0f_{5/2}, 1p_{3/2}, 1p_{1/2})$ (fp) model space. We compare the results for two commonly used Hamiltonians in this model space, GXPF1A [36] and KB3G [37]. We use the shell-model code NuShellX [38]. A calculation of the β strength observed in this experiment requires on the order of 3 000 final states with $J^\pi = (1, 2, 3)^+$. The full fp model-space dimension of 2 292 604 744 J-states for ^{60}Zn is much larger than can be used for calculations. Thus, we explore a series of truncations based upon the number of $0f_{7/2}$ nucleons excited across the $Z = N = 28$ magic number. The simplest of these is to assume that the $0f_{7/2}$ orbital is filled. These are labeled by Δ=0 indicating that no nucleons are excited out of $0f_{7/2}$. For Δ=0 there are 640 J-states for ^{60}Zn, and the decay to all final states can easily be calculated. The results for B(GT) summed up to a given final state energy are shown in Fig.5 Δ=1. All of the results for B(GT) are multiplied by a quenching factor of $(0.774)^2 = 0.55$ from [39] to take into account the average observed differences between experimental GT and theoretical B(GT) observables calculated within the fp model space. This quenching is ascribed to missing nuclear correlations as well as neglected contributions from mesonic-exchange currents [40]. In [41] most of this quenching was reproduced by many-body computations of nuclei based on effective field theories, including an unprecedented amount of correlations in the nuclear wavefunctions.
In addition to Gamow-Teller decay, the β-decay contains a Fermi branch which is observed to the 2^+ T=1 state at 4.85 MeV. This is the IAS of the ^{60}Ga ground state. The main difference between experiment and theory in Fig. 4. is that the IAS energy is too low in the calculation; one MeV too low for GXPF1A and 1.5 MeV too low for KB3G. For all of our calculations the Fermi transition strength (B(F)) is 2 for this Fermi decay.

Next we allow for up to one proton and/or one neutron to be excited out of $0f_{7/2}$. For Δ=1 there are 293 662 J-states for ^{60}Zn, and the decay to about 3 000 final states can be considered. The B(GT) results for Δ=1 are shown by the pink line in Fig.5 Δ=1. There is large change going from Δ=0 to Δ=1 that is due to the addition of the $0f_{7/2}$ to $0f_{5/2}$ "spin-flip" component. This leads to a "giant" Gamow-Teller state near 15 MeV. Strength is removed from the low-lying states into the region of 15 MeV.

Shell-model calculations in heavier nuclei often do not include the orbitals that are required for all of the spin-flip transitions. For example, the region of nuclei from $A = 56 - 100$ are commonly treated in a $(0f_{5/2}, 1p_{3/2}, 1p_{1/2}, 0g_{9/2})$ $(jj44)$ model-space basis. Representative results for the $jj44$ model space obtained with the $jj44b$ Hamiltonian [42] are shown in Fig. 5 Δ=0. The B(GT) below about 10 MeV are reduced about a factor of two compared to the Δ=0. Thus we can expect the effective quenching factor for B(GT) calculated in the $jj44$ model space to be as small as $(0.5)(0.55) = 0.27$.
The largest dimensional calculations we can carry out corresponds to Δ=2 where up to two protons and/or neutrons are excited out of $0f_{7/2}$. For Δ=2 there are 18 201 538 J-states for ^{60}Zn, and the decay to about 1 500 final states can be considered. The B(GT) for Δ=2 results are shown by the purple line in Fig.5 Δ=2. The results for Δ=1 and Δ=2 are similar. This shows that Δ=1 provides a good truncation for the inclusion of the "spin-flip" contributions.

The Δ=1 calculations are compared to experimental results in Fig. 4 and Fig. 6. The shape of the calculations generally agrees with that of the experiment, with the GXPF1A interaction being in better agreement. Both calculations underestimate the strength at high energies.

D. Relativistic proton-neutron QRPA

Relativistic QRPA ((R)QRPA) calculations of the Gamow-Teller strength have been performed in the framework of Ref. [11] which presented a global set of β-decay rates that is now commonly used for astrophysical simulations of the r process. These calculations use the D3C* parametrization of the meson-nucleon Lagrangian [43] for the particle-hole channel of the interaction, and the D1S parametrization of the Gogny force [44] for the like-particle pairing channel.

The Gamow-Teller response, which is generated by the spin-isospin-dependent interaction, also includes

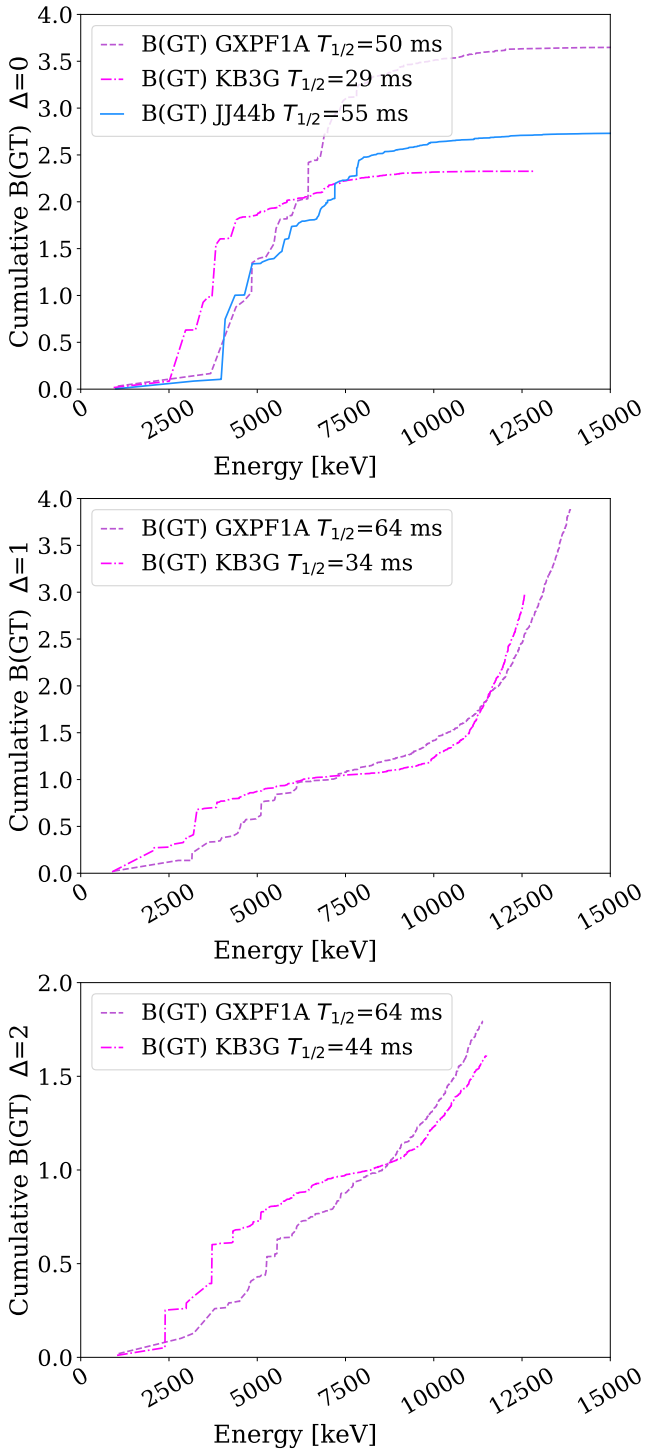

FIG. 5. Gamow-Teller strength calculated for the β-decay of ^{60}Ga (2^+). The results for two Hamiltonians KB3G [37] and GXPF1A [36] are obtained in the fp model space with truncations labeled by Δ as described in the text. In addition, the results with the $jj44b$ Hamiltonian in the $jj44$ model space are shown. Each has the resultant half-life written next to the Hamiltonian name.

pion exchange in the particle-hole component as well as the proton-neutron particle-particle interaction. The pion is included with bare coupling constant and the corresponding contact Landau-Migdal term is adjusted to the experimental Gamow-Teller resonance energy in ^{208}Pb. The isovector proton-neutron particle-particle interaction is determined by isospin symmetry, i.e. it is the same as for the like-particle pairing, while the isoscalar pairing is taken as a Gogny-like form with parameters adjusted to reproduce global β-decay half-lives.

As is often the case in QRPA calculations, the B(GT) distribution, Fig. 6, is found to lack fragmentation compared to the data, as a large part of the strength is concentrated in one single peak and is typically shifted to lower energies. Within this framework we find a β-decay Q-value of 9.16 MeV, about 4.5 MeV less than the β^+ Q-value of 13.56 MeV reported on NNDC. This discrepancy is somehow compensated by the fact that the strength is shifted to lower energies compared to the data, resulting in a calculated half-life of 58.30 ms (obtained without quenching).

We note that here the odd-odd nucleus ^{60}Ga is treated in the same way as even-even nuclei, with a constraint on the number of particles, and is also considered to be spherical. Including the effect of deformation could potentially improve the agreement with the experimental data.

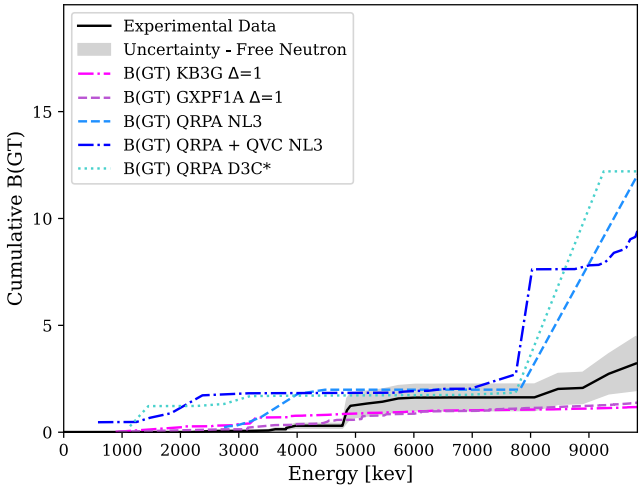

FIG. 6. Comparison of calculated B(GT) from data (black) with various QRPA calculations and Shell Model Hamiltonians. See text for details.

In general, accounting for complex nucleon-nucleon correlations is necessary in order to reproduce the details of the low-energy transition strength that determines β-decay, particularly in the present β^+ channel. This is especially important for nuclei with small Q values. One way to improve the (R)QRPA framework is to include

the coupling between single nucleons and collective vibrations of the nucleus, or quasiparticle-vibration coupling (QVC), which constitutes the leading correlation mechanism in mid-mass and heavy nuclei. In general, this approach has been successful in largely improving GT strength and β-decay half-lives of several nuclei in the β^- channel [45, 46]. We show in Fig. 6 the results obtained without and with such QVC.

These calculations have been done using the NL3 parametrization of the meson-exchange interaction [47] for the particle-hole channel. The isovector pairing interaction is a simple monopole force and the isoscalar pairing is not included. More details can be found in Refs. [45, 48]. The QVC correlations appear to yield fragmentation of the strength distribution, particularly near to the Q value. However, the appearance of strength at very low energy remains. Such shift could potentially be corrected by including consistent QVC effects in the description of the ground state, as was found in studies of doubly-magic nuclei [49], which also improve the Q value. When QVC is included, the half-life is reduced from 127.71 ms to 86.72 ms.

V. CONCLUSIONS

The β^+ decay of ^{60}Ga has been studied using total absorption spectroscopy for the first time at the National Superconducting Cyclotron Laboratory. The half-life of the decay was measured to be 57.7 ± 9.8 ms agreeing with Shell Model calculated half-life of 64 ms for the GXPF1A Hamiltonian as well as some previous experimental measurements [16, 34]. The Gamow-Teller strength distributions and β-feeding intensity, extracted from data, were compared to different theoretical models across a large range of energies. The QRPA models tended to overestimate the strength while the shell model calculations were in good agreement with data, except at high energies. In this nucleus, a β-decay feeding intensity of 12.8% was observed above the proton separation energy of 5.1 MeV compared to 7% for KB3G and 9% for GXPF1A.

We find excellent agreement in B(GT) between the experimental data and the GXPF1A hamiltonian with single particle excitation. The low-energy discrepancies between the other models and data show a need for continued improvement of nuclear models far from stability.

VI. ACKNOWLEDGMENTS

The authors acknowledge support of the operations staff at the National Superconducting Cyclotron Laboratory. The work was supported by the National Science Foundation under grants PHY-1913554, PHY-2209429, PHY 1565546, PHY-1613188, and PHY-2110365. This material is based on work supported by the Department of Energy/National Nuclear Security Administration through the Nuclear Science and Security Consortium under Award No. DE-NA0003180. This material is based upon work supported by the U.S. Department of Energy, Office of Science, Office of Nuclear Physics, under contract number DE-AC02-06CH11357. This work was also supported by the U.S. Department of Energy Office of Science under Grants No. DE-FG02-88ER40387 and DE-SC0019042 and the U.S. National Nuclear Security Administration through Grant No. DE-NA0003909. This work was also partially supported by the Norwegian Research Council under Project No. 262952. This work also received support from the Natural Sciences and Engineering Research Council of Canada (NSERC) S.L. was supported by the Laboratory Directed Research and Development Program at Pacific Northwest National Laboratory operated by Battelle for the U.S. Department of Energy. Part of the theory work was supported by Universität Bielefeld and ERC-885281-KILONOVA Advanced Grant.

[1] J. Grindlay, H. Gursky, H. Schnopper, D. R. Parsignault, J. Heise, A. C. Brinkman, and J. Schrijver, Discovery of intense X-ray bursts from the globular cluster NGC 6624., The Astrophysical Journal L **205**, L127 (1976).

[2] H. Schatz and K. Rehm, X-ray binaries, Nuclear Physics A **777**, 601 (2006), special Isseu on Nuclear Astrophysics.

[3] W. H. G. Lewin, J. van Paradijs, and R. E. Taam, X-Ray Bursts, Space SCience Reviews **62**, 223 (1993).

[4] T. Strohmayer and L. Bildsten, New views of thermonuclear bursts, in *Compact Stellar X-ray Sources*, Cambridge Astrophysics, edited by W. Lewin and M. van der Klis (Cambridge University Press, 2006) p. 113–156.

[5] R. H. Cyburt, A. M. Amthor, A. Heger, E. Johnson, L. Keek, Z. Meisel, H. Schatz, and K. Smith, Dependence of x-ray burst models on nuclear reaction rates, The Astrophysical Journal **830**, 55 (2016).

[6] A. Parikh, J. José, F. Moreno, and C. Iliadis, The effects of variations in nuclear processes on type i x-ray burst nucleosynthesis, The Astrophysical Journal Supplement Series **178**, 110 (2008).

[7] H. Schatz and W.-J. Ong, Dependence of x-ray burst models on nuclear masses, The Astrophysical Journal **844**, 139 (2017).

[8] M. G. Mayer, The shell model, Science **145**, 999 (1964).

[9] J. H. D. Jensen, Nuclear shell models, Rev. Mod. Phys. **29**, 182 (1957).

[10] M. G. Mayer and J. H. D. Jensen, *Elementary Theory of Nuclear Shell Structure* (Wiley, 1955).

[11] T. Marketin, L. Huther, and G. Martínez-Pinedo, Large-scale evaluation of β-decay rates of r-process nuclei with the inclusion of first-forbidden transitions, Phys. Rev. C **93**, 025805 (2016).

[12] S. Lyons, A. Spyrou, S. N. Liddick, F. Naqvi, B. P. Crider, A. C. Dombos, D. L. Bleuel, B. A. Brown, A. Couture, L. C. Campo, J. Engel, M. Guttormsen, A. C. Larsen, R. Lewis, P. Möller, S. Mosby, M. R. Mumpower, E. M. Ney, A. Palmisano, G. Perdikakis, C. J. Prokop, T. Renstrøm, S. Siem, M. K. Smith, and S. J. Quinn, ^{69,71}Coβ-decay strength distributions from total absorption spectroscopy, Phys. Rev. C **100**, 025806 (2019).

[13] A. C. Dombos, A. Spyrou, F. Naqvi, S. J. Quinn, S. N. Liddick, A. Algora, T. Baumann, J. Brett, B. P. Crider, P. A. DeYoung, T. Ginter, J. Gombas, S. Lyons, T. Marketin, P. Möller, W.-J. Ong, A. Palmisano, J. Pereira, C. J. Prokop, P. Sarriguren, D. P. Scriven, A. Simon, M. K. Smith, and S. Valenta, Total absorption spectroscopy of the β decay of ^{101,102}Zr and ^{109}Tc, Phys. Rev. C **103**, 025810 (2021).

[14] J. Gombas, P. A. DeYoung, A. Spyrou, A. C. Dombos, A. Algora, T. Baumann, B. Crider, J. Engel, T. Ginter, E. Kwan, S. N. Liddick, S. Lyons, F. Naqvi, E. M. Ney, J. Pereira, C. Prokop, W. Ong, S. Quinn, D. P. Scriven, A. Simon, and C. Sumithrarachchi, β-decay feeding intensity distributions for ^{103,104m}Nb, Phys. Rev. C **103**, 035803 (2021).

[15] E. Nácher, B. Rubio, A. Algora, D. Cano-Ott, J. L. Taín, A. Gadea, J. Agramunt, M. Gierlik, M. Karny, Z. Janas, E. Roeckl, A. Blazhev, R. Collatz, J. Döring, M. Hellström, Z. Hu, R. Kirchner, I. Mukha, C. Plettner, M. Shibata, K. Rykaczewski, L. Batist, F. Moroz, V. Wittmann, and J. J. Valiente-Dobón, Observations of the gamow-teller resonance in the rare-earth nuclei above ^{146}Gd populated in β decay, Phys. Rev. C **93**, 014308 (2016).

[16] C. Mazzocchi, Z. Janas, J. Döring, M. Axiotis, L. Batist, R. Borcea, D. Cano-Ott, E. Caurier, G. de Angelis, E. Farnea, A. Faßbender, A. Gadea, H. Grawe, A. Jungclaus, M. Kapica, R. Kirchner, J. Kurcewicz, T. Lenzi, S.M.and Martínez, I. Mukha, E. Nácher, D. Napoli, E. Roeckl, B. Rubio, R. Schwengner, T. J.L., and C. Ur, First measurement of β-decay properties of the proton drip-line nucleus 60ga, The European Physical Journal A - Hadrons and Nuclei **12**, 269–277 (2001).

[17] J. Hardy, L. Carraz, B. Jonson, and P. Hansen, The essential decay of pandemonium: A demonstration of errors in complex beta-decay schemes, Physics Letters B **71**, 307 (1977).

[18] E. Nácher, A. Algora, B. Rubio, J. L. Taín, D. Cano-Ott, S. Courtin, P. Dessagne, F. Maréchal, C. Miehé, E. Poirier, M. J. G. Borge, D. Escrig, A. Jungclaus, P. Sarriguren, O. Tengblad, W. Gelletly, L. M. Fraile, and G. L. Scornet, Deformation of the $n = z$ nucleus ^{76}Sr using β-decay studies, Phys. Rev. Lett. **92**, 232501 (2004).

[19] B. C. Rasco, M. Woli ńska Cichocka, A. Fijałkowska, K. P. Rykaczewski, M. Karny, R. K. Grzywacz, K. C. Goetz, C. J. Gross, D. W. Stracener, E. F. Zganjar, J. C. Batchelder, J. C. Blackmon, N. T. Brewer, S. Go, B. Heffron, T. King, J. T. Matta, K. Miernik, C. D. Nesaraja, S. V. Paulauskas, M. M. Rajabali, E. H. Wang, J. A. Winger, Y. Xiao, and C. J. Zachary, Decays of the three top contributors to the reactor $\overline{\nu}_e$ high-energy spectrum, ^{92}Rb, ^{96gs}Y, and ^{142}Cs, studied with total absorption spectroscopy, Phys. Rev. Lett. **117**, 092501 (2016).

[20] D. Morrissey, Planning for a standard in-flight rnb experiment (2003).

[21] D. Bazin, V. Andreev, A. Becerril, M. Doléans, P. Mantica, J. Ottarson, H. Schatz, J. Stoker, and J. Vincent, Radio frequency fragment separator at nscl, Nuclear Instruments and Methods in Physics Research Section A: Accelerators, Spectrometers, Detectors and Associated Equipment **606**, 314 (2009).

[22] A. Simon, S. Quinn, A. Spyrou, A. Battaglia, I. Beskin, A. Best, B. Bucher, M. Couder, P. DeYoung, X. Fang, J. Görres, A. Kontos, Q. Li, S. Liddick, A. Long, S. Lyons, K. Padmanabhan, J. Peace, A. Roberts, D. Robertson, K. Smith, M. Smith, E. Stech, B. Stefanek, W. Tan, X. Tang, and M. Wiescher, Sun: Summing nai(tl) γ-ray detector for capture reaction measurements, Nuclear Instruments and Methods in Physics Research Section A: Accelerators, Spectrometers, Detectors and Associated Equipment **703**, 16 (2013).

[23] A. C. Dombos, A. Spyrou, F. Naqvi, S. J. Quinn, S. N. Liddick, A. Algora, T. Baumann, J. Brett, B. P. Crider, P. A. DeYoung, T. Ginter, J. Gombas, E. Kwan, S. Lyons, W.-J. Ong, A. Palmisano, J. Pereira, C. J. Prokop, D. P. Scriven, A. Simon, M. K. Smith, and C. S. Sumithrarachchi, β-decay half-lives of neutron-rich nuclides in the $a = 100 - 110$ mass region, Phys. Rev. C **99**, 015802 (2019).

[24] S. Agostinelli, J. Allison, K. Amako, J. Apostolakis, H. Araujo, P. Arce, M. Asai, D. Axen, S. Banerjee,

G. Barrand, F. Behner, L. Bellagamba, J. Boudreau, L. Broglia, A. Brunengo, H. Burkhardt, S. Chauvie, J. Chuma, R. Chytracek, G. Cooperman, and et. al, Geant4—a simulation toolkit, Nuclear Instruments and Methods in Physics Research Section A: Accelerators, Spectrometers, Detectors and Associated Equipment **506**, 250 (2003).

[25] S. J. Quinn, *Capture cross sections for the astrophysical p process*, Ph.D. thesis, Michigan State University (2015).

[26] National Nuclear Data Center, Evaluated Nuclear Structure Data File (ENSDF) Retrieval, www.nndc.bnl.gov (2012).

[27] R. Capote, M. Herman, P. Obložinský, P. Young, S. Goriely, T. Belgya, A. Ignatyuk, A. Koning, S. Hilaire, V. Plujko, M. Avrigeanu, O. Bersillon, M. Chadwick, T. Fukahori, Z. Ge, Y. Han, S. Kailas, J. Kopecky, V. Maslov, G. Reffo, M. Sin, E. Soukhovitskii, and P. Talou, Ripl – reference input parameter library for calculation of nuclear reactions and nuclear data evaluations, Nuclear Data Sheets **110**, 3107 (2009), special Issue on Nuclear Reaction Data.

[28] L. Kirsch and L. Bernstein, Rainier: A simulation tool for distributions of excited nuclear states and cascade fluctuations, Nuclear Instruments and Methods in Physics Research Section A: Accelerators, Spectrometers, Detectors and Associated Equipment **892** (2017).

[29] T. Ericson, A statistical analysis of excited nuclear states, Nuclear Physics **11**, 481 (1959).

[30] A. Gilbert and A. G. W. Cameron, A composite nuclear-level density formula with shell corrections, Canadian Journal of Physics **43**, 1446 (1965), https://doi.org/10.1139/p65-139.

[31] S. M. Grimes, J. D. Anderson, J. W. McClure, B. A. Pohl, and C. Wong, Level density and spin cutoff parameters from continuum (p, n) and (α, n) spectra, Phys. Rev. C **10**, 2373 (1974).

[32] J. Kopecky and M. Uhl, Test of gamma-ray strength functions in nuclear reaction model calculations, Phys. Rev. C **41**, 1941 (1990).

[33] F. Naqvi, S. Karampagia, A. Spyrou, S. Liddick, A. Dombos, D. Bleuel, B. Brown, L. Crespo Campo, A. Couture, B. Crider, T. Ginter, M. Guttormsen, A. Larsen, R. Lewis, P. Möller, S. Mosby, G. Perdikakis, C. Prokop, T. Renstrøm, and S. Siem, Total absorption spectroscopy measurement on neutron-rich 74,75cu isotopes, Nuclear Physics A **1018**, 122359 (2022).

[34] S. E. A. Orrigo, B. Rubio, W. Gelletly, P. Aguilera, A. Algora, A. I. Morales, J. Agramunt, D. S. Ahn, P. Ascher, B. Blank, C. Borcea, A. Boso, R. B. Cakirli, J. Chiba, G. de Angelis, G. de France, F. Diel, P. Doornenbal, Y. Fujita, N. Fukuda, E. Ganioğlu, M. Gerbaux, J. Giovinazzo, S. Go, T. Goigoux, S. Grévy, V. Guadilla, N. Inabe, G. G. Kiss, T. Kubo, S. Kubono, T. Kurtukian-Nieto, D. Lubos, C. Magron, F. Molina, A. Montaner-Pizá, D. Napoli, D. Nishimura, S. Nishimura, H. Oikawa, V. H. Phong, H. Sakurai, Y. Shimizu, C. Sidong, P.-A. Söderström, T. Sumikama, H. Suzuki, H. Takeda, Y. Takei, M. Tanaka, J. Wu, and S. Yagi, β decay of the very neutron-deficient ^{60}Ge and ^{62}Ge nuclei, Phys. Rev. C **103**, 014324 (2021).

[35] Kucuk, L., Orrigo, S. E. A., Montaner-Pizá, A., Rubio, B., Fujita, Y., Gelletly, W., Blank, B., Oktem, Y., Adachi, T., Algora, A., Ascher, P., Cakirli, R. B., de France, G., Fujita, H., Ganioğlu, E., Giovinazzo, J., Grévy, S., Marqués, F. M., Molina, F., de Oliveira Santos, F., Perrot, L., Raabe, R., Srivastava, P. C., Susoy, G., Tamii, A., and Thomas, J. C., Half-life determination of tz = -1 and tz = - $\frac{1}{2}$ proton-rich nuclei and the β decay of 58zn, Eur. Phys. J. A **53**, 134 (2017).

[36] M. Honma, T. Otsuka, B. A. Brown, and T. Mizusaki, Effective interaction for pf-shell nuclei, Phys. Rev. C **65**, 061301 (2002).

[37] A. Poves, J. Sanchez-Solano, E. Caurier, and F. Nowacki, Shell model study of the isobaric chains A = 50, A = 51 and A = 52, Nucl. Phys. A **694**, 157 (2001), arXiv:nucl-th/0012077.

[38] B. Brown and W. Rae, The shell-model code nushellx@msu, Nuclear Data Sheets **120**, 115 (2014).

[39] G. Martínez-Pinedo, A. Poves, E. Caurier, and A. P. Zuker, Effective g_A in the pf shell, Phys. Rev. C **53**, R2602 (1996).

[40] I. Towner, Quenching of spin matrix elements in nuclei, Physics Reports **155**, 263 (1987).

[41] P. Gysbers, G. Hagen, J. Holt, G. Jansen, T. Morris, P. Navrátil, T. Papenbrock, S. Quaglioni, A. Schwenk, S. Stroberg, and K. Wendt, Discrepancy between experimental and theoretical β-decay rates resolved from first principles, Nature Physics **15**, 1 (2019).

[42] S. Mukhopadhyay, B. P. Crider, B. A. Brown, S. F. Ashley, A. Chakraborty, A. Kumar, M. T. McEllistrem, E. E. Peters, F. M. Prados-Estévez, and S. W. Yates, Nuclear structure of ^{76}Ge from inelastic neutron scattering measurements and shell model calculations, Phys. Rev. C **95**, 014327 (2017).

[43] T. Marketin, D. Vretenar, and P. Ring, Calculation of β-decay rates in a relativistic model with momentum-dependent self-energies, Phys. Rev. C **75**, 024304 (2007).

[44] J. Berger, M. Girod, and D. Gogny, Time-dependent quantum collective dynamics applied to nuclear fission, Computer Physics Communications **63**, 365 (1991).

[45] C. Robin and E. Litvinova, Nuclear response theory for spin-isospin excitations in a relativistic quasiparticle-phonon coupling framework, Eur. Phys. J. A **52**, 205 (2016).

[46] C. Robin and E. Litvinova, Coupling charge-exchange vibrations to nucleons in a relativistic framework: effect on Gamow-Teller transitions and β-decay half-lives, Phys. Rev. C **98**, 051301 (2018).

[47] G. A. Lalazissis, J. König, and P. Ring, New parametrization for the lagrangian density of relativistic mean field theory, Phys. Rev. C **55**, 540 (1997).

[48] C. E. P. Robin and G. Martínez-Pinedo, Competition between allowed and first-forbidden β decay in r-process waiting-point nuclei within a relativistic beyond-mean-field approach, Phys. Rev. C **110**, 065803 (2024), arXiv:2403.17115 [nucl-th].

[49] C. Robin and E. Litvinova, Time-reversed particle-vibration loops and nuclear Gamow-Teller response, Phys. Rev. Lett. **123**, 202501 (2019).